Electronic Supplementary Material (ESI) for Journal of Materials Chemistry C. This journal is © The Royal Society of Chemistry 2020

Supporting Information

Regioisomeric AIE-active luminogens with substituent aldehyde group for controllable and reversible photochromic behavior and sensitive fluorescent detection of hydrogen sulphite

Hai-Xia Yu, Junge Zhi,* and Jin-Liang Wang*

Key Laboratory of Cluster Science of Ministry of Education, Beijing Key Laboratory of Photoelectronic/Electrophotonic Conversion Materials, School of Chemistry and Chemical Engineering, Beijing Institute of Technology, Beijing, 100081, China.

E-mail: jungezhi@bit.edu.cn; jinlwang@bit.edu.cn

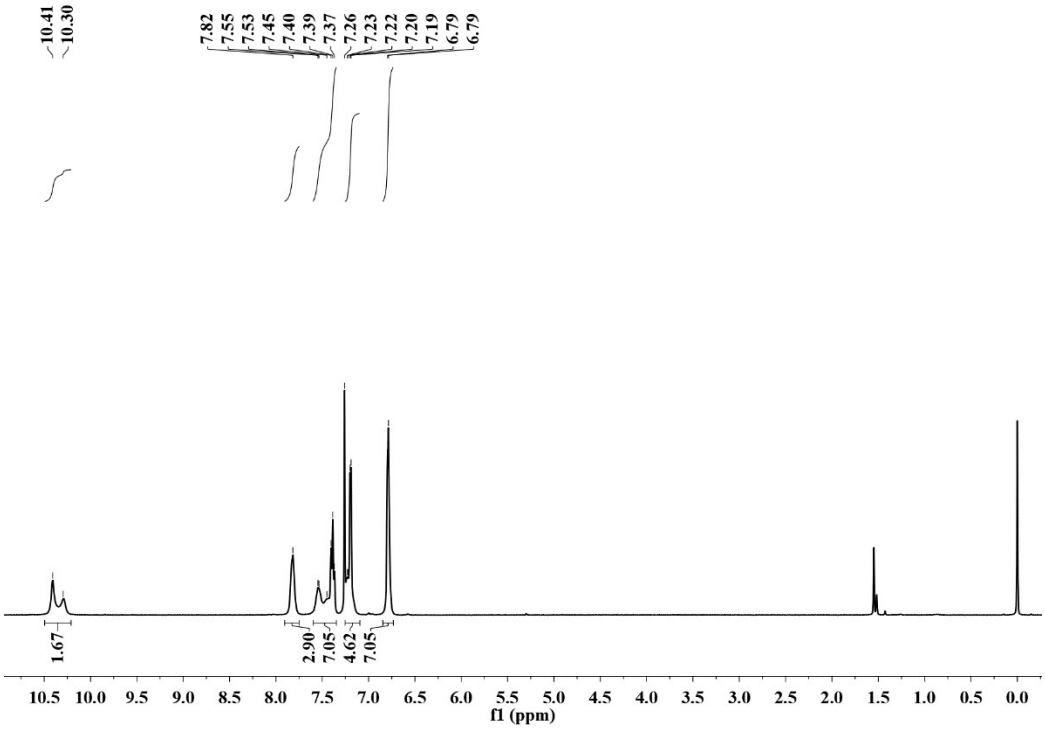

Figure S1. ^{1}H NMR spectrum (in $CDCl_3$) of **DPDT-o-CHO**.

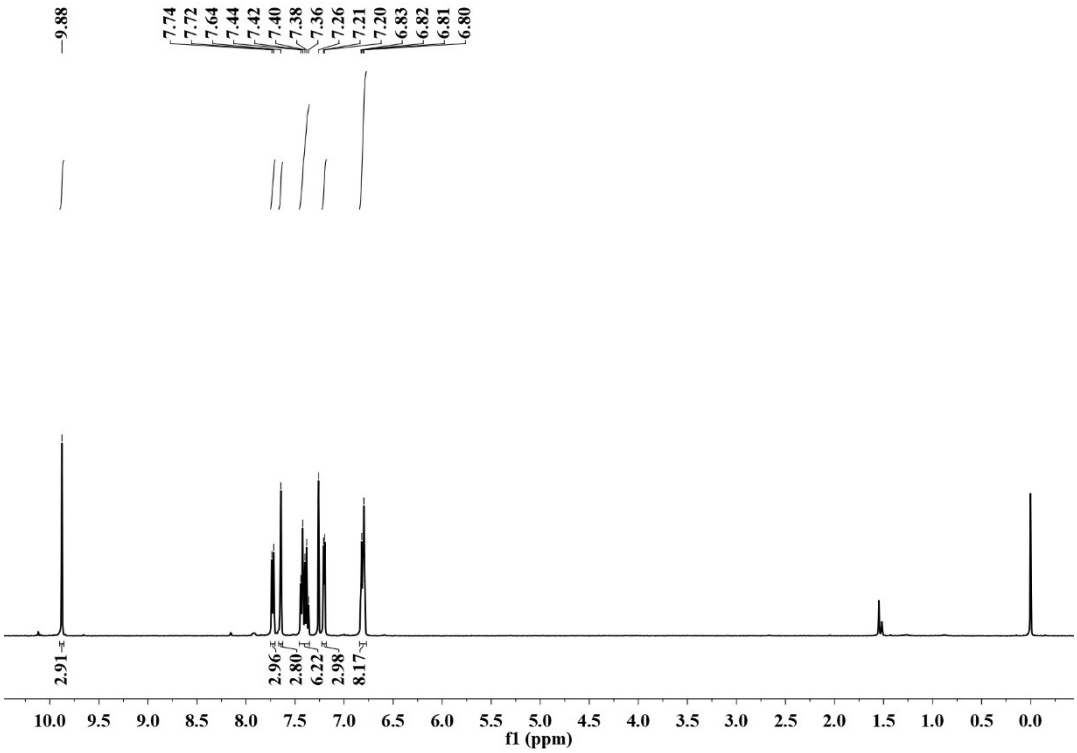

Figure S2. ^{1}H NMR spectrum (in $CDCl_3$) of **DPDT-m-CHO**.

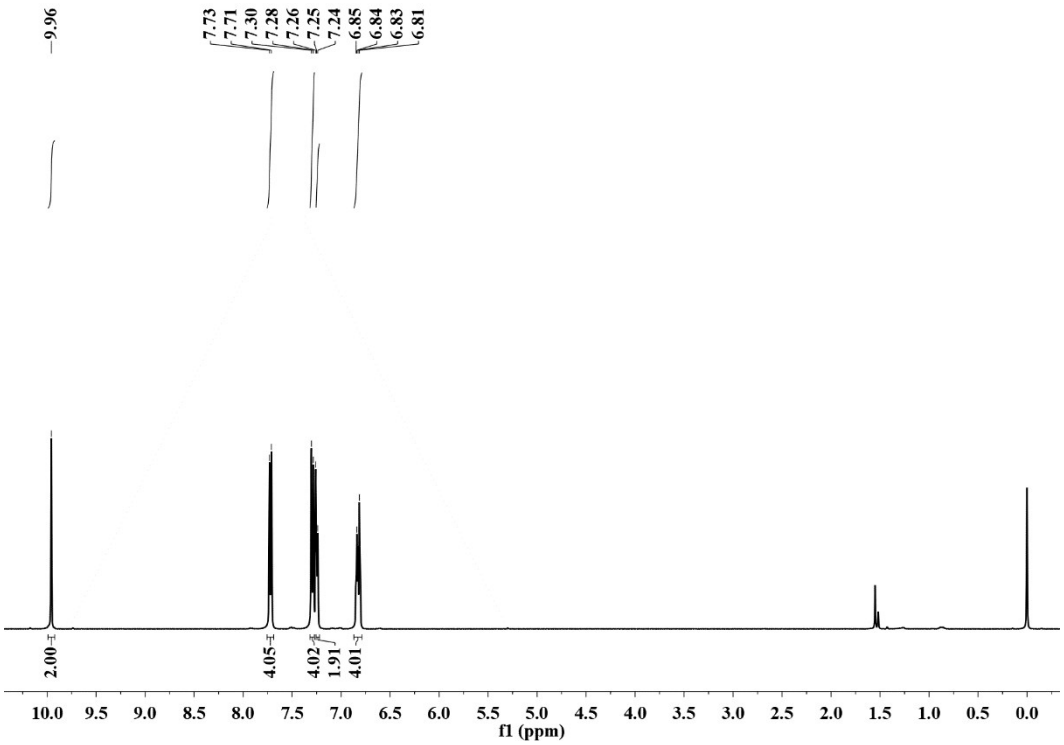

Figure S3. ^{1}H NMR spectrum (in $CDCl_3$) of **DPDT-p-CHO**.

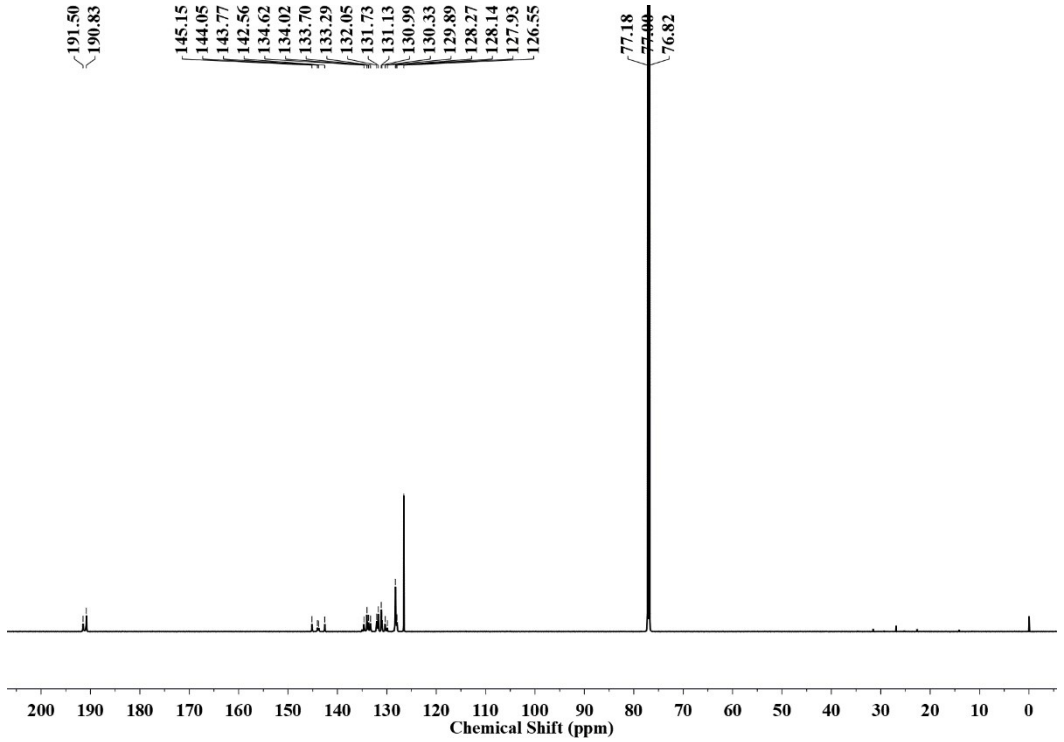

Figure S4. ^{13}C NMR spectrum (in $CDCl_3$) of **DPDT-o-CHO**.

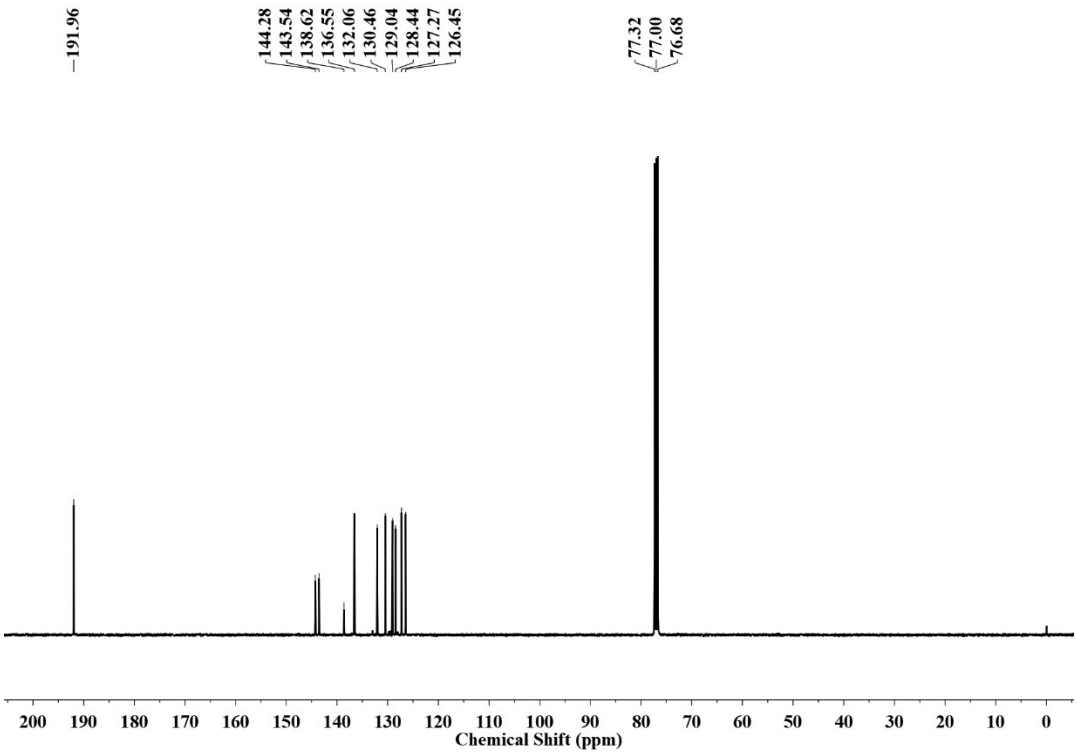

Figure S5. ^{13}C NMR spectrum (in $CDCl_3$) of **DPDT-m-CHO**.

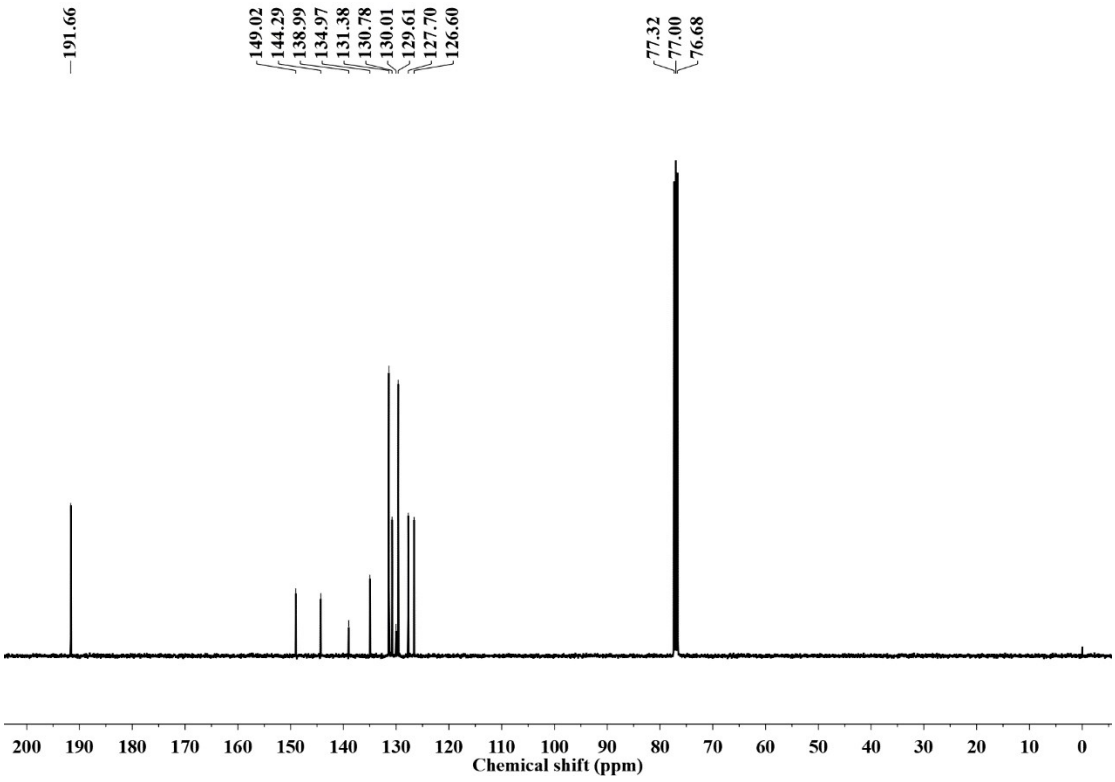

Figure S6. ^{13}C NMR spectrum (in $CDCl_3$) of **DPDT-p-CHO**.

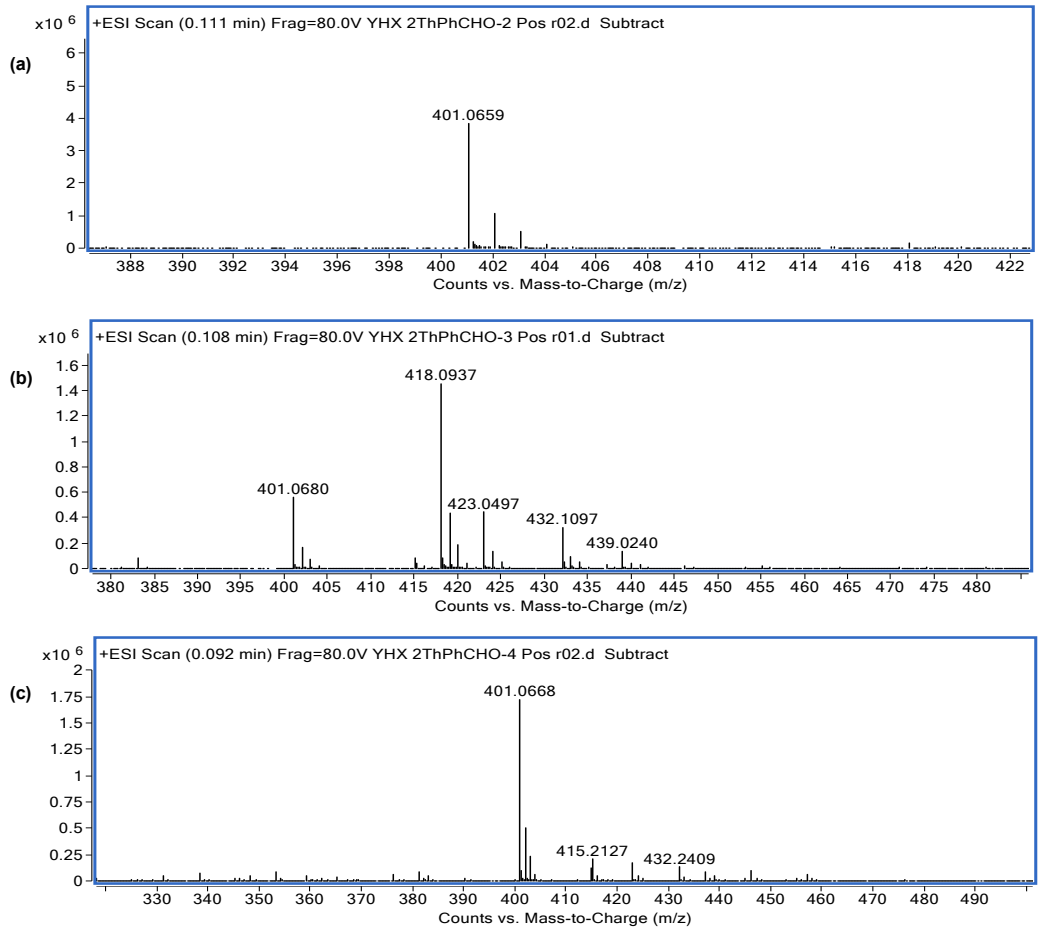

Figure S7. ESI-Mass spectra of (a) **DPDT-o-CHO**, (b) **DPDT-m-CHO** and (c) **DPDT-p-CHO**.

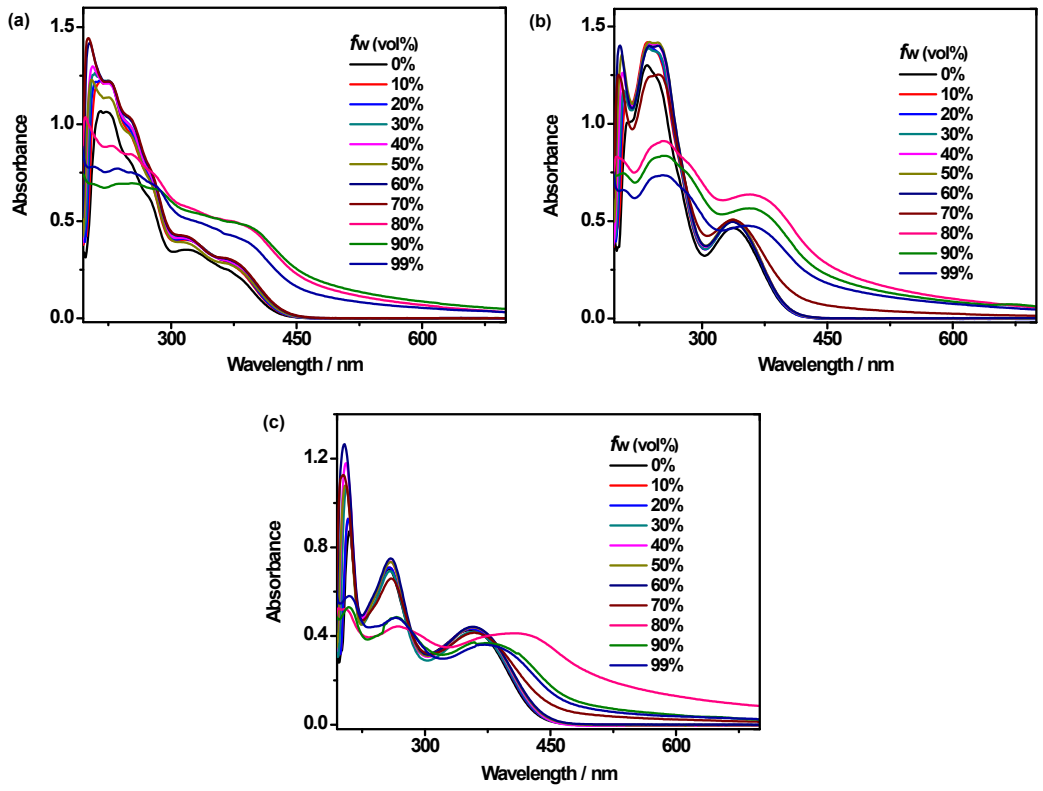

Figure S8. Absorption spectra of (a) **DPDT-o-CHO**, (b) **DPDT-m-CHO** and (c) **DPDT-p-CHO** in CH_3OH-H_2O mixtures with different water contents (f_w).

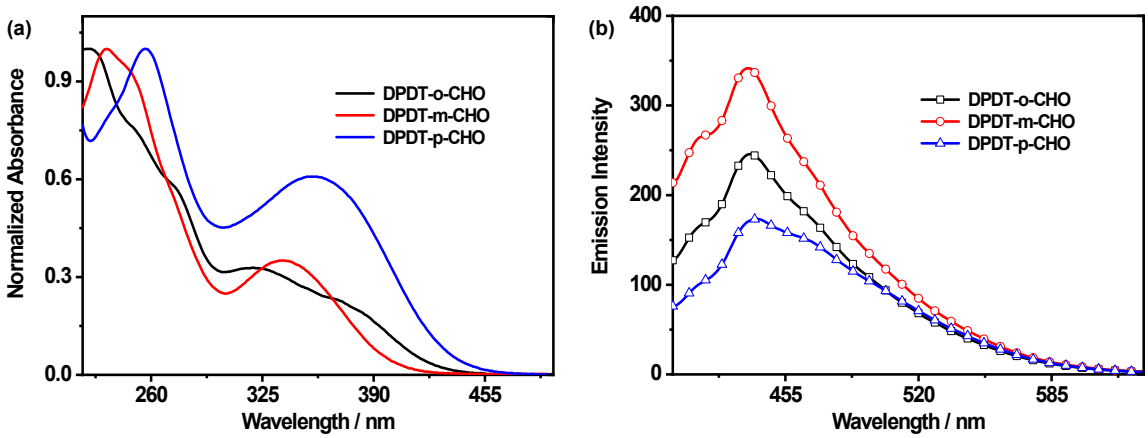

Figure S9. Normalized UV-vis absorption spectra (a) and fluorescence spectra (b) of **DPDT-o-CHO**, **DPDT-m-CHO** and **DPDT-p-CHO** in CH_3OH.

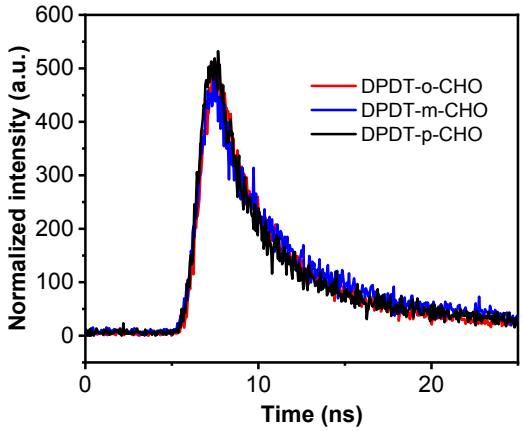

Figure S10. Fluorescence decay spectra of **DPDT-o-CHO**, **DPDT-m-CHO** and **DPDT-p-CHO** in CH_3OH.

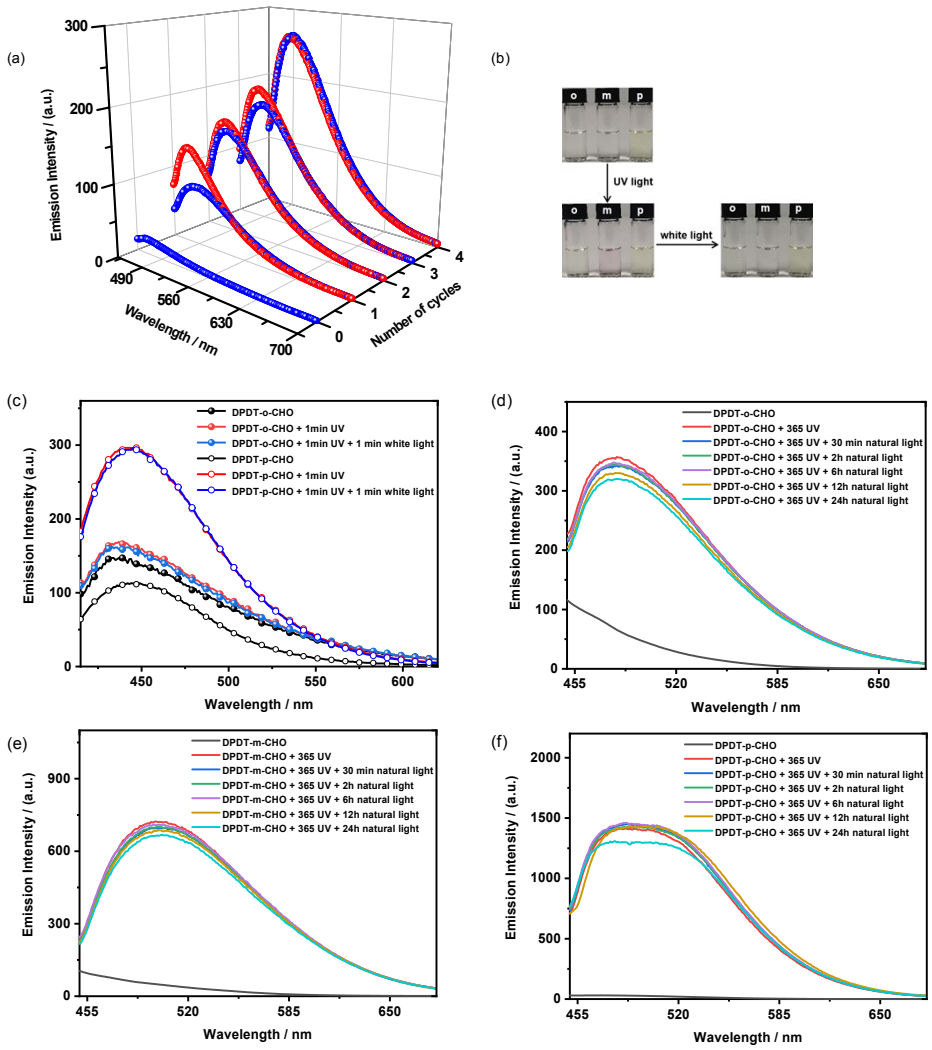

Figure S11. (a) Fluorescence spectra of **DPDT-m-CHO** in CH_3OH in the cycle of 1 min UV irradiation (red line) and 1 min white light (blue line), (b) the photographs of **DPDT-o-CHO** (o), **DPDT-m-CHO** (m) and **DPDT-p-CHO** (p) after the illumination of UV irradiation and white light, (c) **DPDT-o-CHO** and **DPDT-p-CHO** under the UV irradiation (1 min) and white light (1 min), and the fluorescence spectra under the natural light illumination of (d) **DPDT-o-CHO**, (e) **DPDT-m-CHO** and (f) **DPDT-p-CHO** in CH_3OH after 2 h UV-light irradiation.

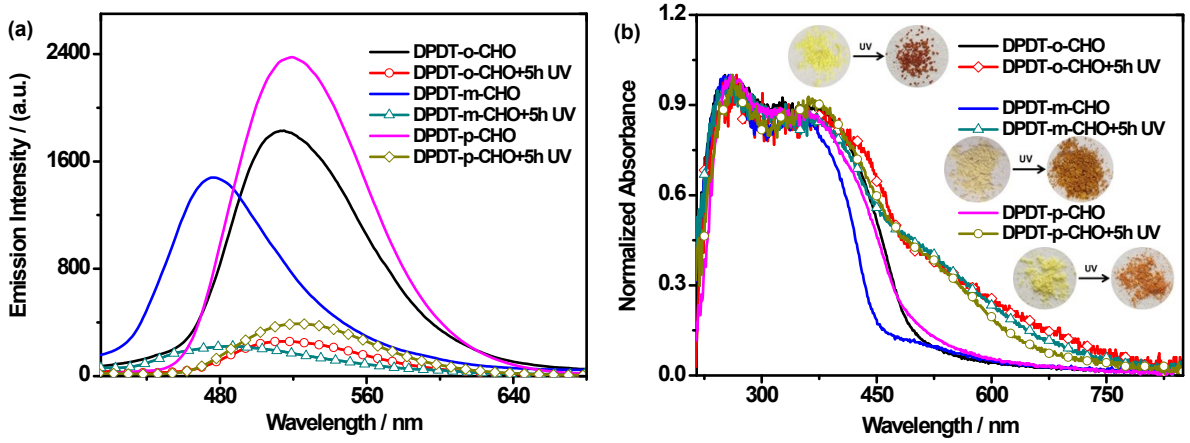

Figure S12. Fluorescence spectra (a) and Normalized absorption spectra (b) of **DPDT-o-CHO**,

DPDT-m-CHO and **DPDT-p-CHO** in solid state before and after UV irradiation for 5 h (The insets show color switch photographs in natural light).

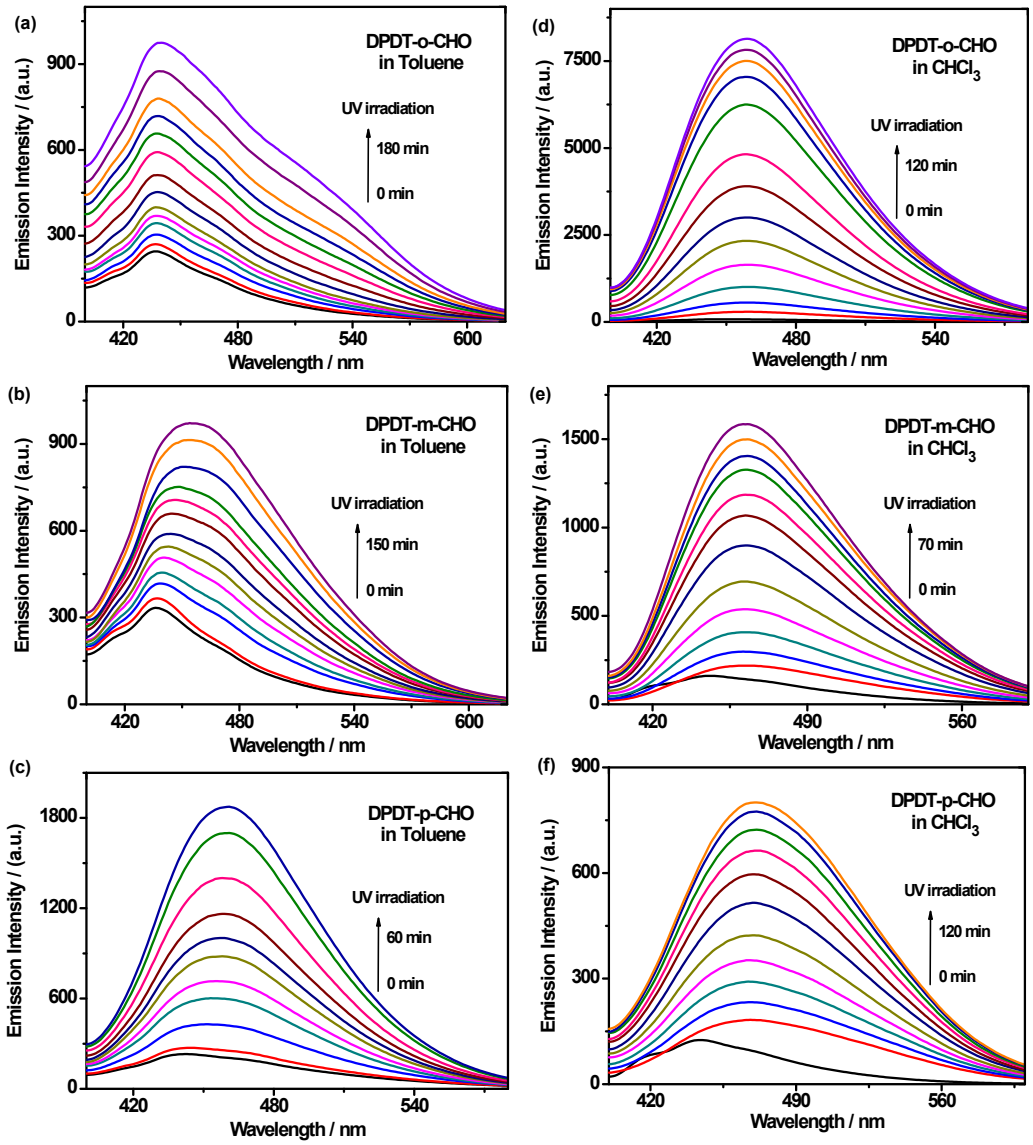

Figure S13. Fluorescence spectra of (a,d) **DPDT-o-CHO**, (b,e) **DPDT-m-CHO** and (c,f) **DPDT-p-CHO** in toluene and $CHCl_3$ upon 365 nm UV irradiation, respectively.

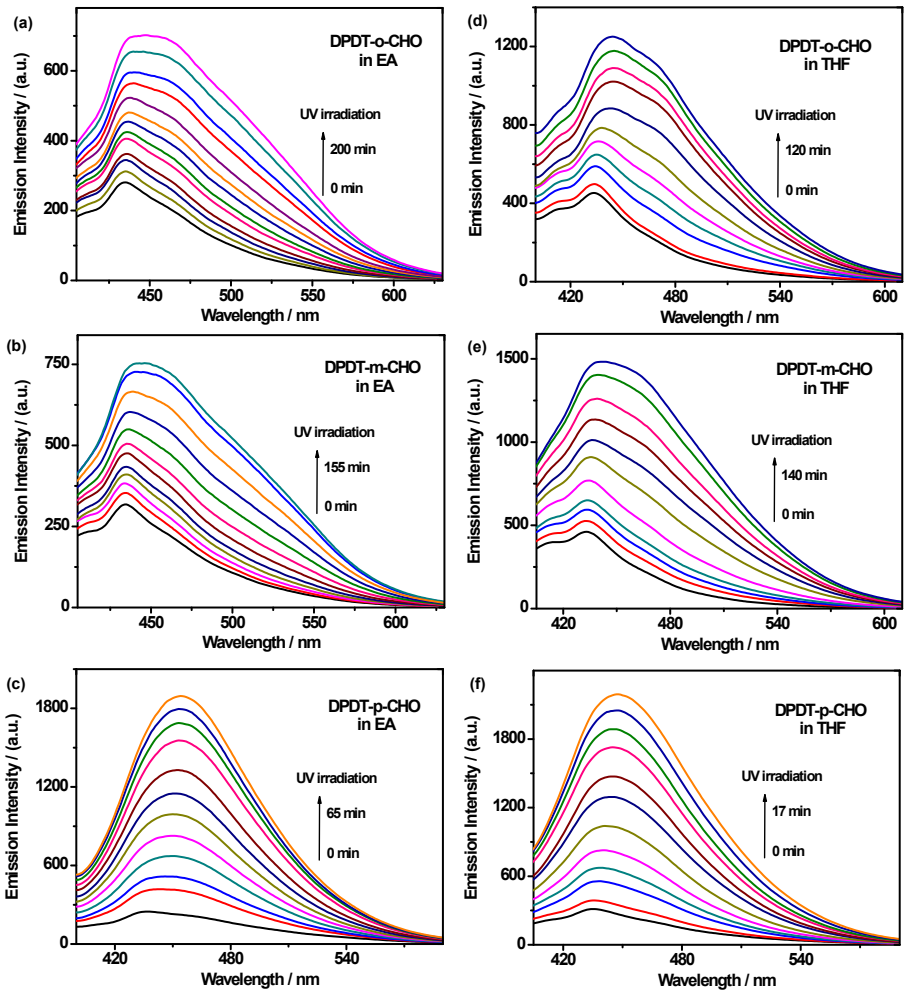

Figure S14. Fluorescence spectra of (a,d) **DPDT-o-CHO**, (b,e) **DPDT-m-CHO** and (c,f) **DPDT-p-CHO** in EA and THF solution upon 365 nm irradiation respectively.

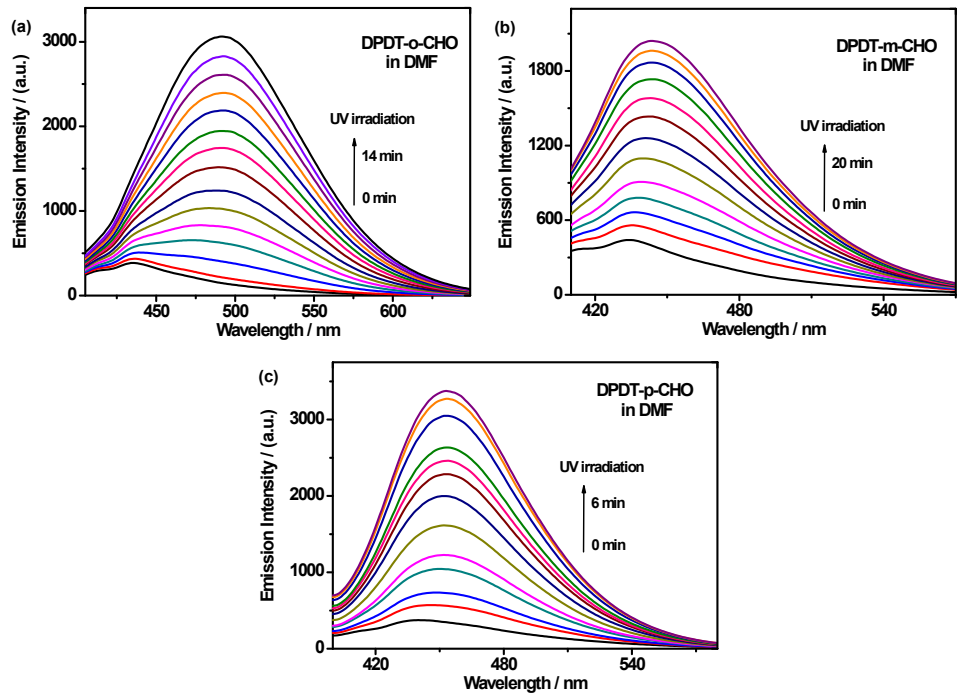

Figure S15. Fluorescence spectra of (a) **DPDT-o-CHO**, (b) **DPDT-m-CHO** and (c) **DPDT-p-CHO** in DMF upon 365 nm irradiation respectively.

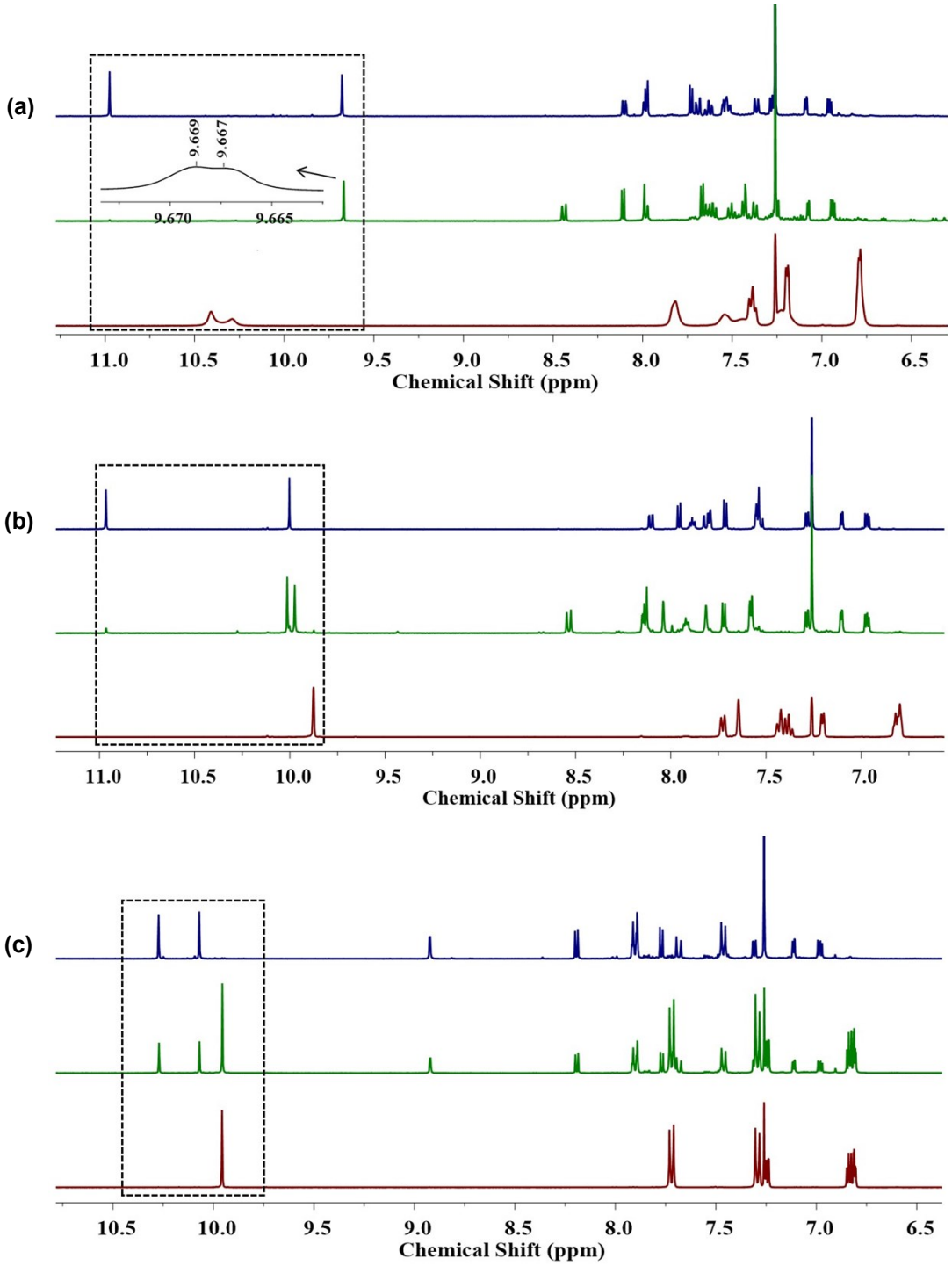

Figure S16. ^{1}H NMR spectra (in $CDCl_3$) of the pristine (red line), upon UV irradiation (green line) and the Katz-modified Mallory photocyclization reaction products (blue line) of (a) **DPDT-o-CHO**, (b) **DPDT-m-CHO**, (c) **DPDT-p-CHO** (The block diagrams focus on the chemical shift of proton signals of -CHO).

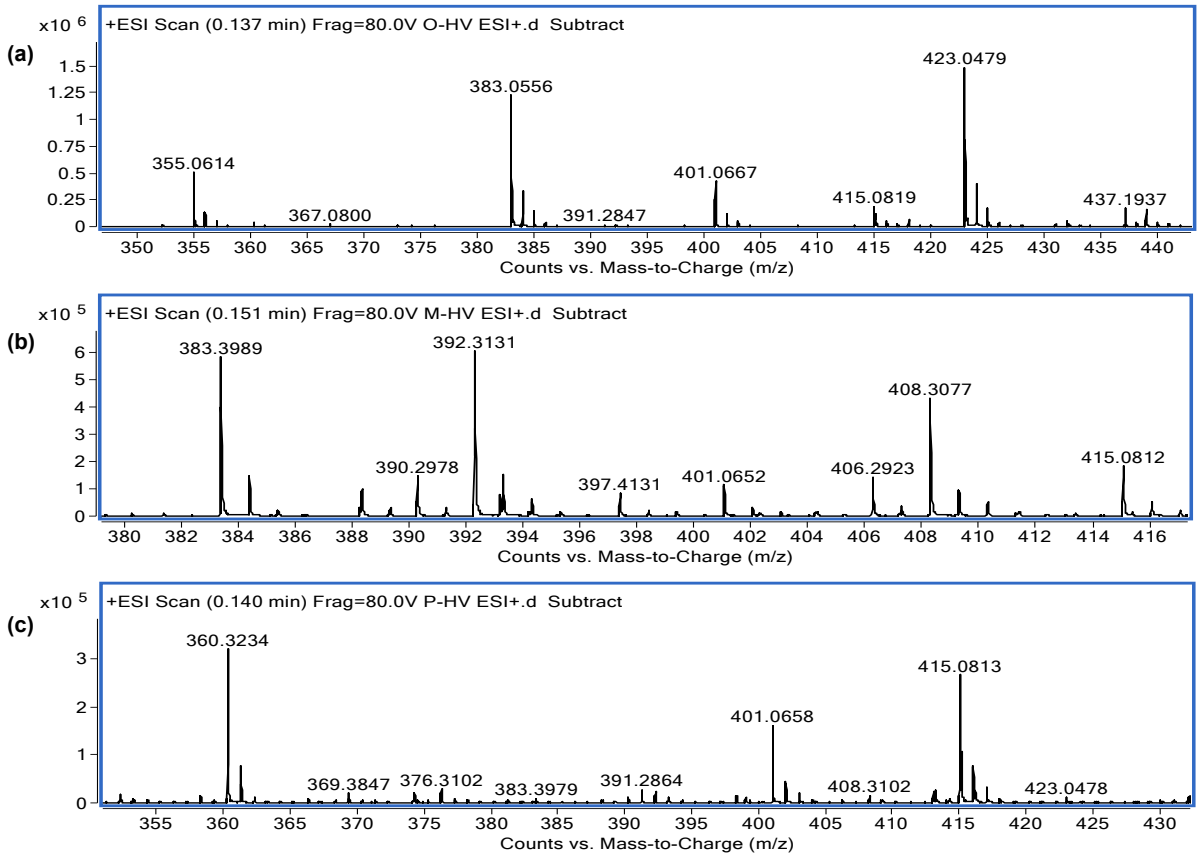

Figure S17. Mass spectra of (a) **DPDT-o-CHO**, (b) **DPDT-m-CHO** and (c) **DPDT-p-CHO** irradiated with UV light in CH_3OH solution.

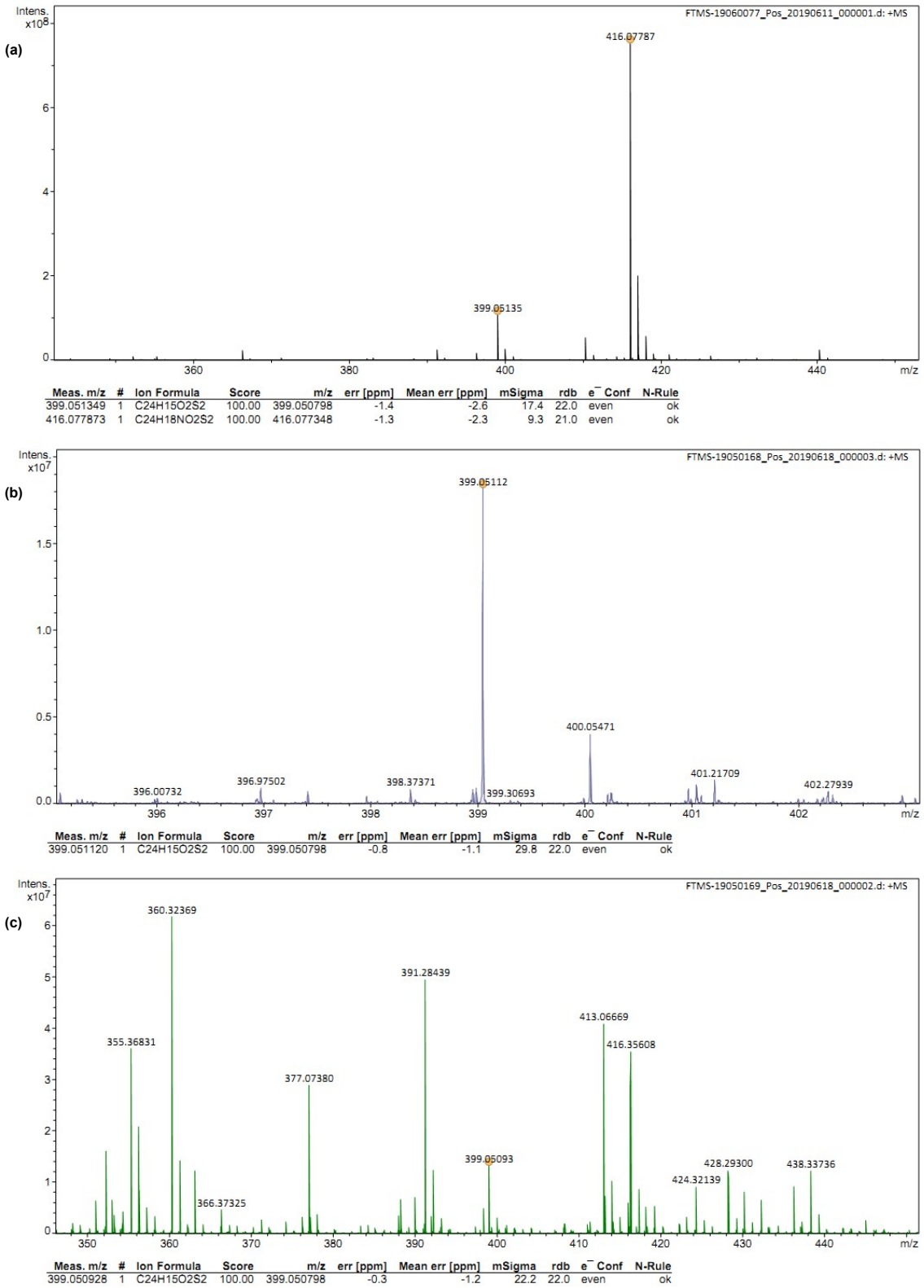

Figure S18. Mass spectra of the Katz-modified Mallory photocyclization reaction products (a) **DPDT-o-CHO (c)**, (b) **DPDT-m-CHO (c)** and (c) **DPDT-p-CHO (c)**.

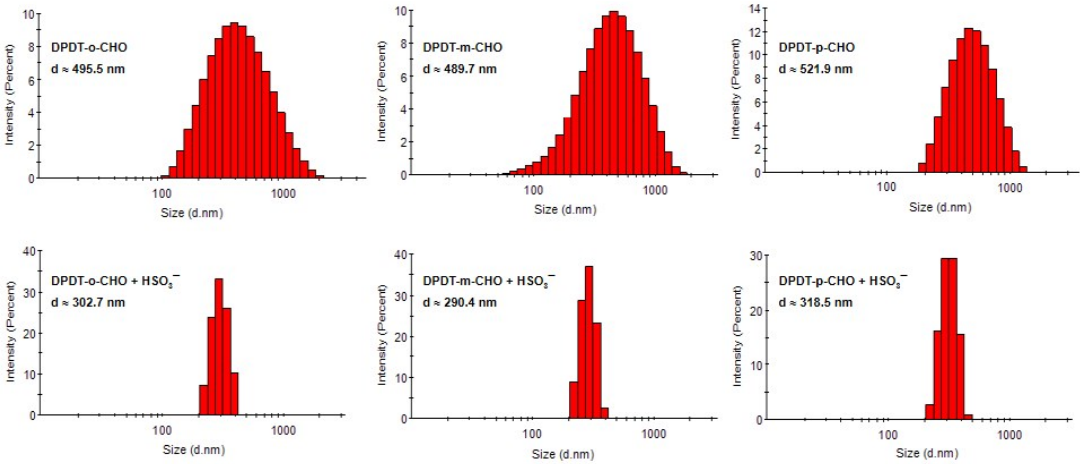

Figure S19. Particle size distributions of the three isomers before and after the addition of HSO_3^- in CH_3OH-H_2O mixture (f_w=90%).

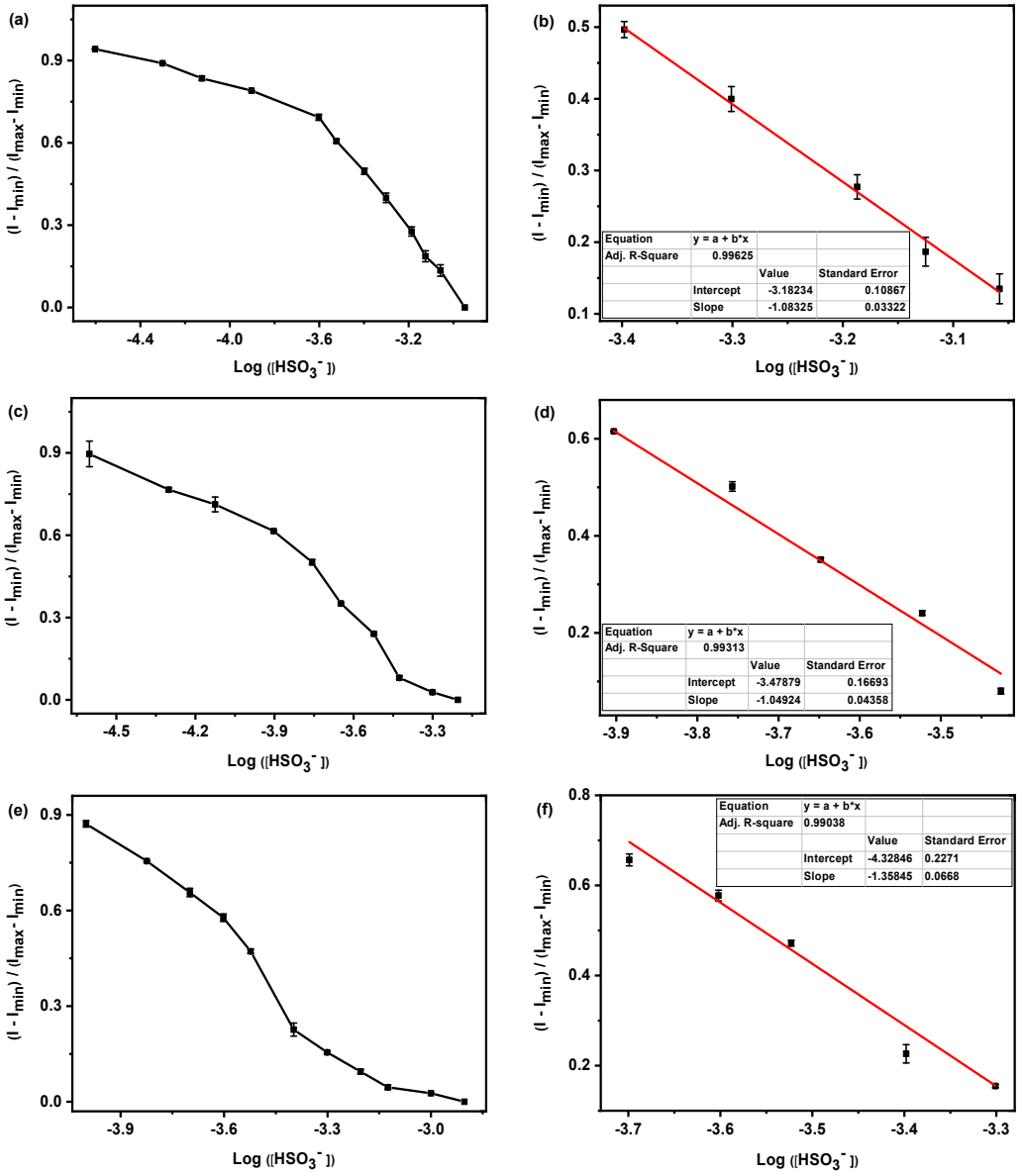

Figure S20. Plots of $(I - I_{min})/(I_{max} - I_{min})$ versus log $[HSO_3^-]$ and linear fitting for (a,b) **DPDT-o-CHO**, (c,d) **DPDT-m-CHO** and (e,f) **DPDT-p-CHO**.

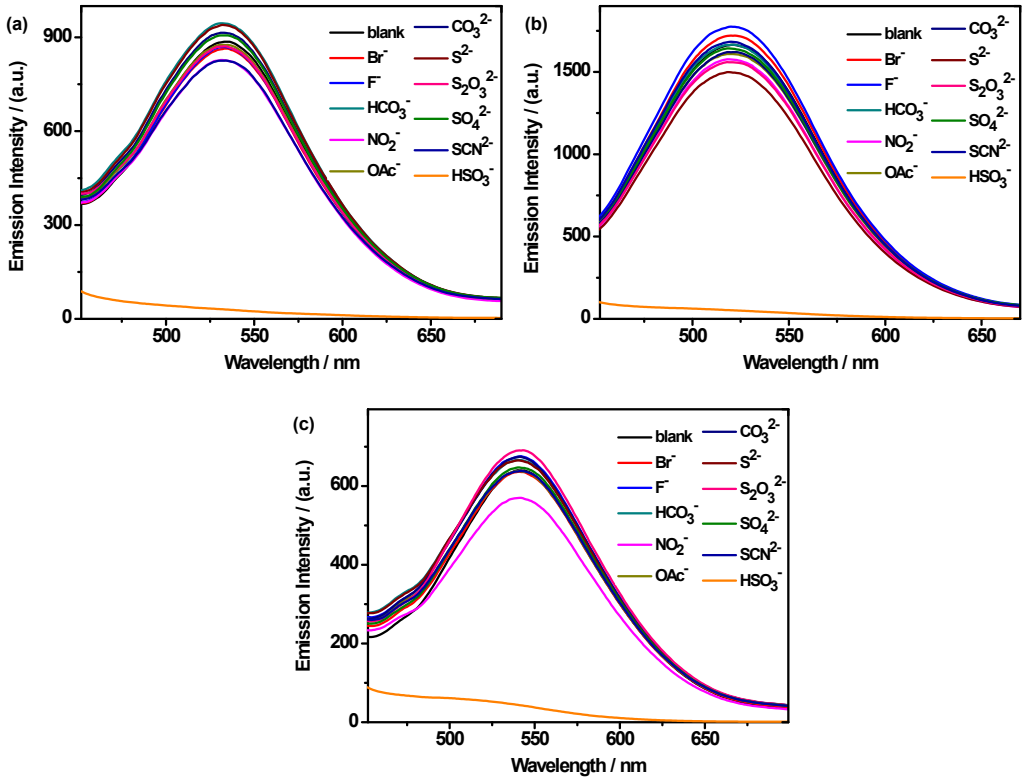

Figure S21. Fluorescence spectra of (a) **DPDT-o-CHO**, (b) **DPDT-m-CHO**, (c) **DPDT-p-CHO** responding to various anions (100 equiv.)

Table S1. List of sing-crystal X-ray diffraction data for **DPDT-o-CHO**, **DPDT-m-CHO** and **DPDT-p-CHO** (CCDC 1911367, 1911368 and 1911369).

Compound		**DPDT-o-CHO**	**DPDT-m-CHO**	**DPDT-p-CHO**
Temperature		296 K	296 K	296 K
Bond precision		C-C = 0.0060 Å	C-C = 0.0090 Å	C-C = 0.0040 Å
		Wavelength = 0.7107 Å	Wavelength = 0.0090 Å	Wavelength = 0.71073 Å
Cell	a (Å)	6.4405(5)	9.5360(14)	9.5258(6)
	b (Å)	10.8836(8)	9.7981(15)	21.9137(13)
	c (Å)	14.5616(11)	13.849(3)	9.9541(6)
	α (°)	98.145(2)	108.993(5)	90
	β (°)	91.900(3)	94.411(6)	102.602(2)
	γ (°)	91.005(3)	92.833(5)	90
Volume		1009.60(13)	1216.1(4)	2027.8(2)
Crystal system		triclinic	triclinic	monoclinic
Space group		P -1	P -1	P21/n
Hall group		-P 1	-P 1	-P 2yn
Formula		$C_{24}H_{16}O_2S_2$	$C_{24}H_{16}O_2S_2$	$C_{24}H_{16}O_2S_2$
Molecular		400.49	400.49	400.49

Weight			
Dx, g cm^{-3}	1.317	1.291	1.312
Z	2	2	4
μ (mm^{-1})	0.280	0.246	0.279
F000	416.0	496.0	832.0
h, k, lmax	7, 12, 17	12, 13, 18	12, 29, 13
Nref	3545	5962	5046
Data completeness	0.998	0.989	0.995
Theta(max)	24.996	28.275	28.360
R(reflections)	0.0827(2719)	0.0993(2088)	0.0771(3654)
wR2(reflections)	0.2821(3545)	0.3740(5962)	0.2754(5046)
S	1.080	1.004	1.046
Npar	254	275	264